



Modeling and Optimization of Flux Assisted Tungsten Inert Gas Welding Process Using Taguchi Method and Statistical Analysis

M. Azadi Moghaddam, F. Kolahan*

Department of Mechanical Engineering, Ferdowsi University of Mashhad, Mashhad, Iran

ABSTRACT: Flux assisted tungsten inert gas welding process known as activated tungsten inert gas welding process is being extensively used in order to improve the performance of tungsten inert gas welding process. In this paper, welding current, welding speed and welding gap have been considered as process input variables in fabricating of AISI316L austenitic stainless steel parts. Depth of penetration and weld bead width have been taken in to account as process response parameters. In this paper SiO₂, Nano-particles have been considered as an activating flux. To gather required data for modeling and optimization purposes, Taguchi method has been employed. Then, process response parameters have been measured and their corresponding signal to noise ratios have been calculated. Next, different regression equations have been applied on signal to noise ratio values and the most fitted ones have been selected. Furthermore, welding current has been determined as the most important parameter affects depth of penetration and weld bead width with 68% and 88% percent contribution respectively. Next, signal to noise analysis, in such a way that weld bead width minimized and depth of penetration is maximized has been used. Finally, experimental performance evaluation tests have been carried out, based on which it can be concluded that the proposed procedure is quite efficient (with less than 7% error) in modeling and optimization of the process.

Review History:

Received: 2019-08-08
Revised: 2019-11-06
Accepted: 2019-12-09
Available Online: 2019-12-11

Keywords:

Modeling
Depth of penetration
Weld bead width
Design of experiments
Signal to noise analysis

1. INTRODUCTION

Nowadays, Gas Tungsten Arc Welding (GTAW), also known as Tungsten Inert Gas (TIG) welding is one of the most widely used welding processes for fabricating stainless steels parts due to its good quality and surface finish. As TIG welding process produces a shallow penetration, its application for fabricating of thick parts in a single pass has been restricted [1-3]. To cope with this problem different procedures has been introduced among which hybrid welding (e.g. Laser-TIG) and Activated TIG (A-TIG) welding processes are the most important ones [4,5].

Laser-TIG hybrid butt joint welding process parameters have been investigated using Response Surface Methodology (RSM) by Moradi et al. [6]. Welding speed, welding current and distance of heat sources have been considered as input process variables. Furthermore, the weld surface width, weld seam area, and weld penetration were assumed as the process responses. Results of ANalysis Of VAriance (ANOVA) indicated that the welding speed is the most important parameter. The desirability approach has also been utilized for optimization purpose.

Effect of hybrid laser – TIG welding variables (TIG current, laser power, pulse frequency, pulse duration) on the process responses (Depth Of Penetration (DOP) and Weld Bead Width (WBW)) for welding of AISI316LN have been investigated by

*Corresponding author's email: kolahan@um.ac.ir

Ragavendran et al. [7]. Central Composite Design (CCD) has been employed to design the experimental matrix required for gathering data. To correlate the process variables with the responses, regression modeling procedure has been used. For optimization purpose, the desirability approach has been employed. Then, determined process optimum variables have been validated using confirmation experiments. Based on the results, there was a good agreement between the predicted and measured values.

Mechanical and metallurgical properties of dissimilar welding (SS400 low carbon steel to AISI304) in hybrid laser-TIG welding process have been investigated by Chen et al. [8]. Based on the results, when the heat sources have been placed on the interface of welding materials, the weld quality has been improved as compared to having an offset to the stainless steel or carbon steel sides. Microstructure, tensile strength, and hardness were strongly determined by the location of heat sources in the process due to the disparity of thermal behaviors developing in two welding materials.

Using hybrid welding requires special equipment which results in increase the cost of production. To tackle this problem A-TIG welding process has been introduced. This process can be taken in to account as the TIG welding process in which a layer including activating fluxes used on the weld surface before welding process started. These fluxes, are melted and vaporized during the process and due to arc constriction



and reversal of Marangoni convection phenomena, depth of penetration and weld bead width are increased and decreased respectively [1,2].

A-TIG welding process has been effectively employed on different materials namely: alloy steels, stainless steels including austenite and austenite duplex stainless steels, and dissimilar metals welding [9-11]. Application of A-TIG welding process, allowed steel parts (of around 10 mm) to be welded with single pass welding without even using filler metal and edge preparation [9].

A-TIG welding process has been used by Kumar et al. [12] to tackle the drawback of poor penetration in TIG welding process of thick plates and pipes. Results have shown, full penetration has been achieved using A-TIG welding process in comparison with conventional TIG welding process. Venkatesan et al. [13] has reported using A-TIG welding process eliminates edge preparation and reduces the numbers of welding passes needed for accomplishing fabricating. Mechanical properties improvement and reduction of distortion were introduced by Chern et al. [14] as the main assets of the A-TIG welding process. Different fluxes (including oxide, chloride, and fluoride fluxes) have been employed by Tathgir and Bhattacharya [15] in A-TIG welding process of stainless steels and low alloy parts to improve *DOP*. Based on the research results, using oxide fluxes results in the largest *DOP* in comparison with other fluxes.

There are different studies in which A-TIG welding process has been considered. Nonetheless, to the best of our knowledge, there is no published study in which modeling and optimization of *DOP* and *WBW* are considered using Orthogonal Array Taguchi (OA-Taguchi) method for designing experimental matrix, mathematical modeling (regression) for establishing the relationships between process input variables and process response parameters, statistical analysis (ANOVA) to determine the most fitted models and significant parameters, and Signal to Noise (*S/N*) approach for optimization of process response parameters (*DOP* and *WBW*). Therefore, in this article, three process inputs

variables (welding current (*I*), welding speed (*S*) and welding gap (*G*)) has been taken into account. Moreover, *DOP* and *WBW* have been considered as process response parameters. In the proposed approach, experimental test matrix gathered base on the OA-Taguchi method. Regression modeling has been performed to establish a relation between process input variables and process response parameters. Then, in order to choose the most fitted derived regression equations as the authentic representatives of the process, ANOVA technique has been performed. Furthermore, significance of the process input variables and their corresponding percent contribution (68% and 88% percent contribution reported for welding current affects *DOP* and *WBW* respectively) on the process response parameters measures have been determined based on the ANOVA results. Next, in order to maximize *DOP* and minimize *WBW* signal to noise (*S/N*) analysis has been used.

2.EXPERIMENTAL SET-UP

To carry out the experiments, a welding machine (DIGITIG 250 AC/DC) equipped with an automatic bed has been used. Furthermore, Argon (with 99.7% purity) as welding shield gas has been used. AISI316L stainless steel sheets (100 mm×50 mm×10 mm) have been considered as specimens. Chemical composition of the material used has been presented in Table 1. In this study, SiO₂ Nano-powder has been used as the activating flux. The powdered oxide used has an average particle size of 20-30 nm with 99% purity.

Prior to welding, 1000 mg of flux powder was mixed with 2 ml of carrier solvent (ethanol), and the mixture was stirred using a glass rod in a beaker until a paste-like flux attained. Then, the flux was coated on the specimen with a brush. Upon evaporation of the carrier solvent, the flux layer remained attached to the surface of the specimen. Fig. 1 illustrates the preparation process of the paste-like flux [2].

2.1. Process input variables and their corresponding levels

Welding current (*I*), speed (*S*) and gap (*G*) are the most noticeable parameters in A-TIG welding process which have

Table 1. Chemical composition of AISI316L

AISI	C	Mn	P	S	Si	Cr	Ni	Mo
316L	0.03	2.0	0.05	0.04	1.0	17.3	13.6	2.7

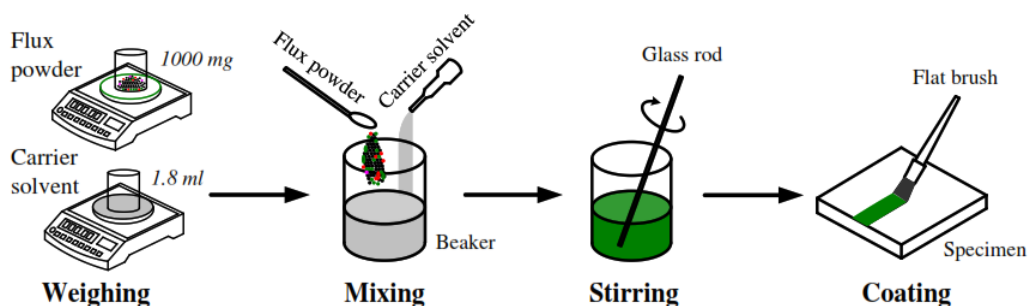


Fig. 1. Activating flux preparation procedure [2]

Table 2. A-TIG welding process input variables and their levels

Welding parameters	welding gap (G)	Welding current (I)	Welding speed (S)
Unit	mm	Amps	mm/sec
Symbol	G	I	S
Interval	0.75-1.50	100-280	1.00-3.00
Level 1	0.75	100	1.00
Level 2	1.50	160	1.67
Level 3	-	220	2.34
Level 4	-	280	3.00

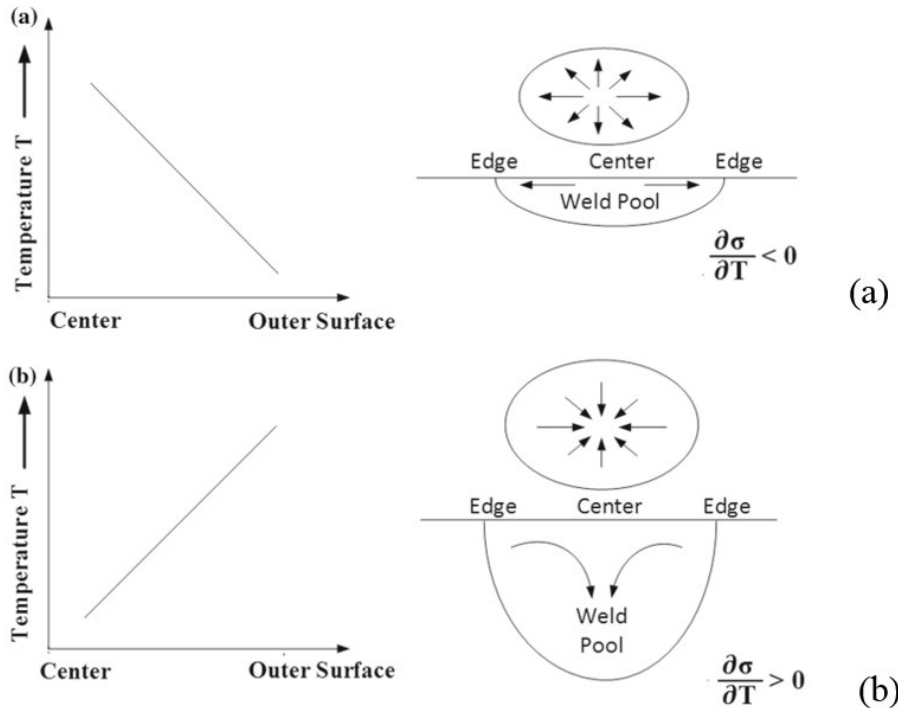


Fig. 2. Schematic illustration of Marangoni convection [18]
(a) Marangoni convection in conventional TIG welding process
(b) Reversal of Marangoni convection in A-TIG welding process

been considered in this study as the process input variables [1-3]. Similarly, *DOP* and *WBW* are the most important process responses of A-TIG welding process. To determine the possible working intervals of each process input variables, welding references studied and some preliminary tests were conducted [13-15]. Table 2, lists the process input parameters and their corresponding intervals and levels. Other input parameters with trivial effects have been considered at a fixed level.

2.2. Design of experiments

After selecting the process input variables and their intervals and levels, an appropriate design matrix for conducting the required experiments have to be determined. Generally, Design Of Experiment (DOE) approach is used to facilitate the identification of the influence of individual parameters, establish the relationships between process input variables and response parameters, and finally determine the optimal levels of input parameters in order to get the desired process responses. one of the effective methods that

can intensely reduce the number of experiments required to gather necessary data is OA-Taguchi method [16]. An OA-Taguchi's L_{32} design matrix has been chosen based on the number of input parameters and their levels.

2.3. Experimental results

The fluid flow mode of molten metal in weld pool determines the size and shape of the weld bead in the welding process. Generally, fluid flow and surface tension of the weld pool have been affected by the heat of the welding arc. At the center of weld pool the surface tension compared to the outer edges, is minimum, therefore, the surface tension gradient is negative ($(\partial\sigma/\partial T) < 0$) [17]. Thus, The Marangoni convection, acts in a direction from center toward weld periphery. Molten mass flows from the center of weld pool towards the weld periphery results in a shallow and wide weld pool. During A-TIG welding process, the top surface of the specimen is covered with paste-like powder flux. The presence of oxygen, as a surface active element in molten metal reverses the

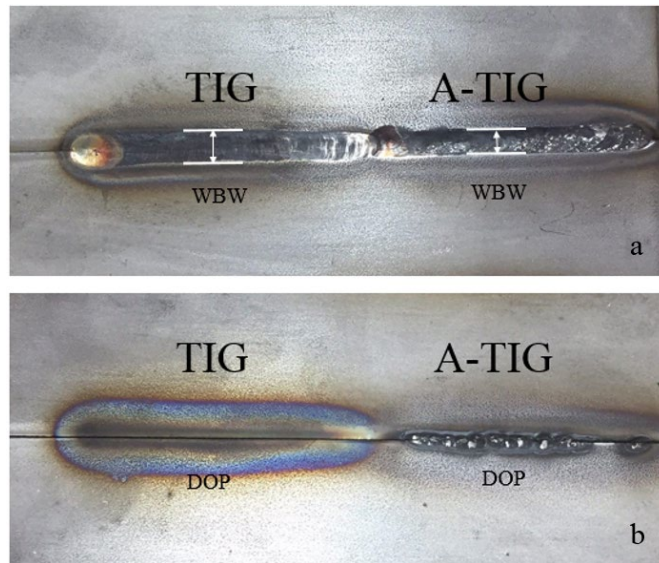


Fig. 3. Comparison of the process responses of conventional TIG and A-TIG welding processes
(a) Full penetration, for both TIG and A-TIG welding processes
(b) Incomplete penetration, for both TIG and A-TIG welding processes

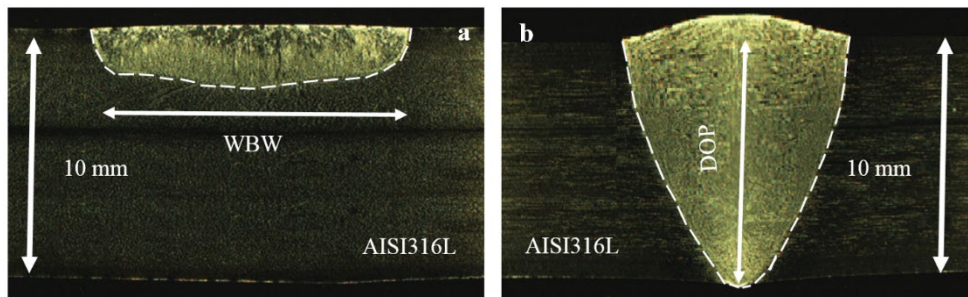


Fig. 4. Comparison of TIG and A-TIG weldments cross sections under the same welding condition (10X)
(a) Incomplete penetration using TIG welding process
(b) Full penetration using A-TIG welding process

Marangoni convection, which changes the direction of the surface tension gradient from the boundary of weld pool towards the center; therefore, the surface tension gradient becomes positive ($(\partial\sigma/\partial T) > 0$). This phenomena results in an increase in penetration and reduction in welding width. In Fig. 2 the schematic illustration of the phenomena has been shown [18]. Fig. 2(a), represents the Marangoni convection in conventional TIG welding process, which results in a wide and shallow weld bead. In the same token, Fig. 2(b), illustrates the reversal of Marangoni convection in A-TIG welding process using which improve the performance of TIG welding process due to increase of *DOP*.

In TIG welding of AISI316L stainless steel specimens produced without flux, the delta-ferrite content increased from 1.2 *FN* of base metal to 6.1 *FN* due to solidified as delta-ferrite phase [18]. During welding, the cooling rate of the weld metal is so rapid that the phase transformation of delta-ferrite to austenite do not complete. Consequently, more delta-ferrite retained in the weld metal after solidification. On the other hand, when using oxide fluxes, the delta-ferrite content in activated TIG weld metal slightly increased to 7.0–7.6 *FN*.

This result is related to the heat input during A-TIG welding. It is also found that the arc voltage increases when the A-TIG process is used. Since the calculated heat input is proportional to the measured arc voltage, applied activated flux has the positive effect of increasing the heat input unit length of welds. Because this higher heat input can increase the peak temperature of the welds, and consequently, more delta-ferrite forms in the A-TIG weld metal. All cases exhibited a microstructure of austenite matrix and vermicular delta-ferrite morphology typical of this class of material [16,19].

The results showed that the oxide flux did not produce a significant change the hardness of AISI316L weldments. The austenite has an Face-Centered Cubic (FCC) crystal structure. The delta-ferrite has a Body-Centered Cubic (BCC) crystal structure. The BCC structure has a higher mechanical strength than that of the FCC structure. When A-TIG is used, the delta-ferrite content in the weld metals is increased, and has a beneficial effect in increasing the hardness of AISI316L weldments [19].

In A-TIG welding process based on reversal of Marangoni convection and arc constriction phenomena, the WBW will

Table 3. Experimental conditions based on Taguchi method and their measured outputs and S/N ratios

No.	Welding gap (mm)	Welding current (Amp)	Welding speed (mm/sec)	DOP (mm)	WBW (mm)	S/N value for DOP	S/N value for WBW
1	0.75	100	1.00	2.97	4.10	21.7712	-28.2197
2	0.75	100	1.67	2.71	4.19	19.9390	-28.6540
3	0.75	100	2.34	2.32	3.75	16.8313	-26.4351
4	0.75	100	3.00	2.33	3.96	16.7213	-27.0151
5	0.75	160	1.00	5.15	6.39	32.7799	-37.0947
6	0.75	160	1.67	4.40	5.46	29.6321	-33.9490
7	0.75	160	2.34	3.52	5.35	25.1692	-33.5419
8	0.75	160	3.00	3.20	5.20	23.2630	-32.9732
9	0.75	220	1.00	7.75	7.82	40.9539	-41.1337
10	0.75	220	1.67	5.42	7.10	33.8019	-39.2019
11	0.75	220	2.34	4.65	7.30	30.7373	-39.7575
12	0.75	220	3.00	4.45	6.94	29.8581	-38.7460
13	0.75	280	1.00	9.15	9.65	44.2751	-45.3392
14	0.75	280	1.67	7.10	9.45	39.2019	-44.9203
15	0.75	280	2.34	5.80	9.07	35.1572	-44.0994
16	0.75	280	3.00	4.83	9.43	31.4969	-44.8779
17	1.50	100	1.00	2.66	4.80	19.8202	-31.1245
18	1.50	100	1.67	2.60	4.95	19.1102	-31.9878
19	1.50	100	2.34	2.20	4.10	15.7691	-28.2197
20	1.50	100	3.00	1.91	4.12	12.9421	-28.3171
21	1.50	160	1.00	5.77	6.50	35.0534	-37.4360
22	1.50	160	1.67	4.08	7.07	28.1219	-39.1172
23	1.50	160	2.34	3.39	5.50	24.4166	-34.0950
24	1.50	160	3.00	3.06	5.42	22.3683	-33.8019
25	1.50	220	1.00	7.82	8.78	41.1337	-43.4495
26	1.50	220	1.67	6.13	9.32	36.2639	-44.6433
27	1.50	220	2.34	4.67	7.58	30.8232	-40.5103
28	1.50	220	3.00	4.11	7.37	28.2685	-39.9484
29	1.50	280	1.00	11.02	10.39	47.9942	-46.8169
30	1.50	280	1.67	8.52	11.05	42.8483	-48.0486
31	1.50	280	2.34	5.95	9.76	35.6678	-45.5658
32	1.50	280	3.00	4.70	9.31	30.9532	-44.2433

be reduced, therefore, Heat Affected Zone (HAZ) will be smaller in comparison to conventional TIG welding process. Moreover, rapid solidification results in smaller grain size. Smaller HAZ and grain size will be ended in higher corrosion resistance in this process.

To increase the accuracy, experiments have been conducted in random orders. After welding, two process response parameters (DOP and WBW) have been taken from each sample. Fig. 3, displays specimens that have been fabricated under the same welding condition (same variable levels) for both conventional TIG (left side of the Fig. 3) and A-TIG (right side of the Fig. 3) welding processes. As shown, A-TIG welding process results in smaller WBW and higher DOP. Fig. 3(a), represents a condition of welding under which a full penetration has been achieved for both TIG and A-TIG welding processes. Furthermore, the WBW in A-TIG welding process was smaller than TIG welding process. In the same way, Fig. 3(b), illustrates a condition for which penetration is incomplete for the both processes. However, for A-TIG welding process more penetration has been reported.

For measuring DOP and WBW, on each samples two

transverse cross sections were made. Next, to clearly show DOP and WBW, the cut faces were smoothly polished and etched (Fig. 4). A stereo microscope M 80 (with zoom magnification of 7.5x - 60x and 2.34x - 120x for total magnification with additional, ATM Co.) has been used to measure the DOP and WBW. Fig. 4(a), illustrates a cut face which has smoothly polished and etched after welding by TIG welding process. Full penetration for A-TIG welding process has been presented by Fig. 4(b).

Then, for taking images an optical microscope has been used. To determine samples DOP and WBW, images were consequently processed by Microstructural Image Processing (MIP) software. The average of two measurements for each sample was reported in Table 3.

3. SIGNAL TO NOISE ANALYSIS

Experimental matrix based on DOP approach is used by OA-Taguchi method to study the whole process input parameters space with small numbers of experiments. Taguchi method also uses signal to noise ratios as performance measures to optimize the process response parameters. To

Table 4. ANOVA results of different models for the A-TIG welding process characteristics

Model	Variable	R ²	R ² (adj)	F-value	Pr>F
Linear	DOP	95.7%	95.2%	185.90	<0.0001
logarithmic	DOP	92.2%	91.6%	152.83	<0.0001
Second order	DOP	99.4%	99.2%	489.21	<0.0001
Linear	WBW	95.7%	95.4%	258.86	<0.0001
logarithmic	WBW	92.6%	92.0%	161.88	<0.0001
Second order	WBW	98.1%	97.8%	271.16	<0.0001

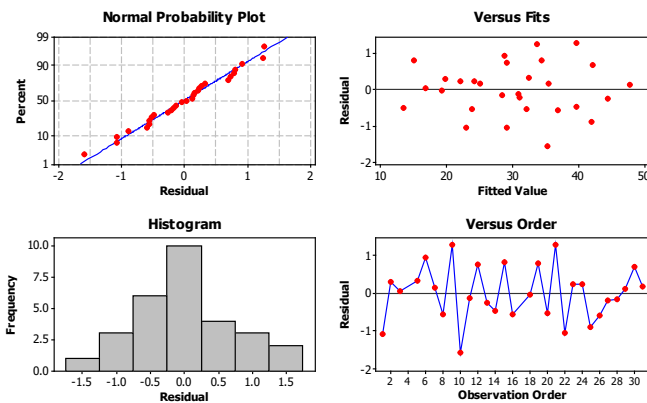


Fig. 5. Residual plot for depth of penetration (DOP)

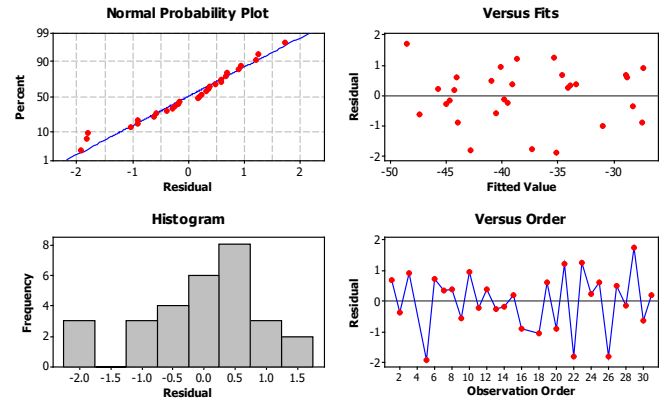


Fig. 6. Residual plot for weld bead width (WBW)

Table 5. Result of ANOVA for S/N of Depth of Penetration

Welding parameters	Degree of freedom (Dof)	Sum of square (SS)	Mean Square	F-Value	Percent contribution (%)
G	1	0.40	0.40	0.17	1
I	3	1605.2	535.09	226.40*	68
S	3	677.60	225.87	95.57*	29
Error	24	56.72	2.36	-	2
Total	31	2340.00	-	-	100

Significant Parameter *

calculate the deviation between the experimental and desired value, a loss function is introduced. The loss function is transformed into S/N ratio. The S/N ratio calculation may be decided as “Smallest is the Best, (SB)” or “Largest is the Best, (LB)” based on the process under consideration, as given in Eqs. (1) and (2) [20].

$$SB: S/N(\eta) = -10 \log \left(\frac{1}{n} \sum_{k=1}^n X_k^2 \right) \quad (1)$$

$$LB: S/N(\varphi) = -10 \log \left(\frac{1}{n} \sum_{k=1}^n \frac{1}{X_k^2} \right) \quad (2)$$

where number of iteration in a trial shown as n , in this study, $n=1$ and x_k is the j^{th} measured value in a run. Therefore, as the lowest WBW and the highest DOP are desired, Eqs. (1) and (2) are considered to calculate WBW and DOP respectively. The experimental results of 32 experiments and their corresponding S/N ratio values based on the Taguchi

method are reported in Table 3.

4. REGRESSION MODELING AND ANALYSIS OF VARIANCE

Regression modeling is a statistical procedure for approximating the relationships between process input variables and response parameters. To carry out this procedure the following stages are to be taken in to account [21,22].

The first three columns of Table 2 are the process input variables. The next two columns are the measured process responses (DOP and WBW) based on the conducted experiments in each rows. The last two columns are the calculated S/N ratio values for the measured responses. Any of the above output is a function of process parameters which are expressed by linear, logarithmic and second order functions; as stated in Eqs. (3) to (5) respectively [22].

$$Y_1 = a_0 + (a_1 \times B) + (a_2 \times C) + (a_3 \times D) \quad (3)$$

Table 6. Result of ANOVA for S/N of Weld Bead Width

Welding parameters	Degree of freedom (Dof)	Sum of square (SSj)	Mean Square	F-Value	Percent contribution (%)
G	1	31.48	31.48	12.70	2
I	3	1369.90	456.63	184.26*	88
S	3	103.18	34.39	13.88*	7
Error	24	59.48	2.48	-	3
Total	31	1564.04	-	-	100

Significant Parameter *

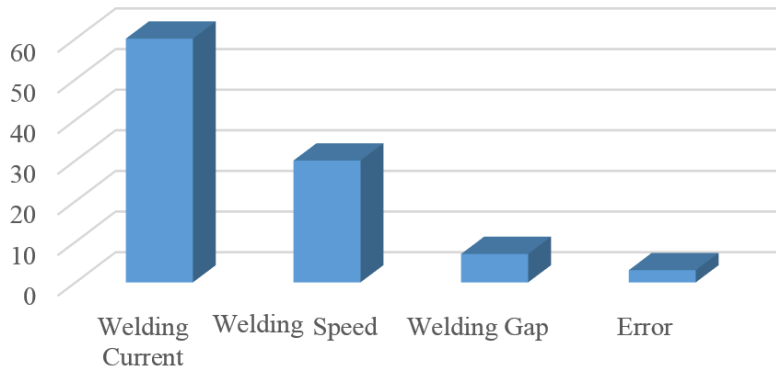


Fig. 7. Percent contributions of welding parameters to the DOP

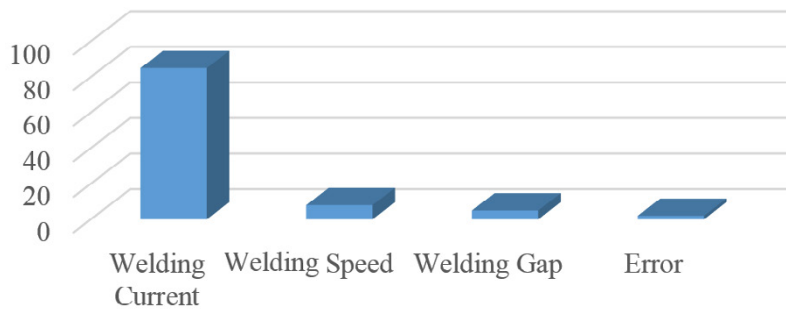


Fig. 8. Percent contributions of welding parameters to the WBW

$$Y_2 = a_0 + (a_1 \times B) + (a_2 \times C) + (a_3 \times D) + (a_{11} \times B \times B) + (a_{22} \times C \times C) + (a_{33} \times D \times D) + (a_{12} \times B \times C) + (a_{13} \times B \times D) + (a_{23} \times C \times D) \quad (4)$$

$$Y_3 = a_0 \times B^{a_1} \times C^{a_2} \times D^{a_3} \quad (5)$$

where, regression constants are shown with a_0, a_1, a_2 and a_3 and are to be predicted. Furthermore, B, C and D are the input parameters (I, S, G) and Y_1, Y_2 and Y_3 are the process response parameters (S/N ratio values for DOP and WBW). Based on the calculated S/N ratios for DOP s and WBW s data given in Table 2, the regression equations are developed using MINITAB software.

To determine how well a model fits the experimental data and represents the authentic process under study ANOVA is performed [23]. ANOVA procedure within 95% of confidence limit has been employed to check the adequacies of proposed regression models (Table 4) [18].

Obviously, Eqs. (6) and (7), the second order model (with elimination of unimportant parameters) for DOP and

WBW are the superior models to other models based on the required confidence limit (P_r), the correlation factor (R^2) and the adjusted correlation factor (R^2-adj). Thus, these superior models are considered as the best authentic representative of the A-TIG welding process in this paper.

$$S/N(DOP) = 6.82 + (0.243 \times I) - (5.08 \times S) - (0.000329 \times I \times I) + (1.13 \times S \times S) + (0.0221 \times G \times I) - (1.74 \times G \times S) - (0.0138 \times I \times S) \quad (6)$$

$$S/N(WBW) = -13.1 - (5.68 \times G) - (0.136 \times I) + (0.000125 \times I \times I) + (1.41 \times G \times S) - (0.00182 \times I \times S) \quad (7)$$

The residual plots for DOP and WBW have been shown in Figs. 5 and 6 respectively. This figures demonstrate a good conformability of the developed model to the real process (normal probability plot). Moreover, histogram plots show the normal distribution of the residuals. Based on the residual-fitted value plots, there is no pattern to be followed by the residuals. Furthermore, order of observation versus residuals

Table 7. Response (mean) of S/N values for depth of penetration

Symbol	Level 1	Level 2	Level 3	Level 4
G	29.47433	29.47216	-	-
I	17.86305	27.60055	33.98006	38.44933
S	35.4727	31.1149	26.82146	24.48393

Table 8. Response (mean) of S/N values for weld bead width

Symbol	Level 1	Level 2	Level 3	Level 4
G	-36.6224	-38.5828	-	-
I	-28.7466	-35.2511	-40.9238	-45.4889
S	-38.8268	-38.8153	-36.2404	-36.5281

Table 9. Results of optimization based on the Taguchi method

parameters	Set of Parameters			Predicted S/N value	Experimental S/N value	Error (%)	
		G	I				S
Taguchi optimization	Setting Levels for optimized DOP	1.50	280	1.00	46.0517	43.1270	6.3
	Setting Level for optimized WBW	0.75	100	3.00	-27.0133	-28.8160	6.7

show that the residual changes is accidentally.

The detailed results of ANOVA for S/N values of DOP and WBW have been illustrated in Tables 4 and 5. As showed large F-value illustrates that the variation of the process parameter makes a big change on the performance of the process. In this study, to evaluate parameters significances a 95% confidence level is selected. Therefore, F-values of A-TIG process parameters are compared with the appropriate values from confidence Table, F_{α, ν_1, ν_2} ; where α is risk, degrees of freedom associated with numerator and denominator illustrated in Tables 5 and 6 are shown by ν_1 and ν_2 [21]. Within a confidence limit of 95%, ANOVA results show that welding current, welding speed and welding gap are respectively the most important input parameters affecting DOP and WBW.

The percent contributions of each parameter may be provided by ANOVA results (Eq. (8)) [22]. The percent contributions of the A-TIG process parameters are shown in Figs. 7 and 8.

$$P_i (\%) = \frac{SS_i - (DOF_i \times MS_{error})}{\text{Total Sum of Square}} \quad (8)$$

where, P_i is percentage of contribution for each parameters under consideration, SS_i is sum of square, DOF_i is degree of freedom of i^{th} factor, and MS_{error} is mean sum of square of error [22].

According to Fig. 7, welding current is the major factor affecting DOP at 68% contribution. It is followed by welding speed at 29%. Welding gap has a trivial effect on DOP (at 1% contribution). The rest (2%) is due to error and uncontrollable parameters. Based on the nature of the process and the equipment used, it is acceptable. By the same token, welding

current with 88%, welding speed with 7% and welding gap with 2% are the most important parameters affecting WBW respectively.

5. TAGUCHI BASED OPTIMIZATION METHOD

To define the effect of each process input variables on the process response parameters, the mean of S/N ratios for each test containing this parameter in desired level are calculated. Moreover, the calculated means for each level of input parameter under consideration are compared and the level to which the highest value belongs considered as the desired level in order to optimize the process characteristic [21]. For example mean effect of welding speed in level 1 is gained from averaging test runs number 1, 2 up to 16. Along these lines, the mean effects of parameters are computed and listed in Tables 7 and 8.

Since the higher value of mean S/N is favorable, with respect to the data in Table 4 optimal set of parameters for optimization of DOP are: G at level 1, I at level 4 and S at level 1. Similarly, optimal set of parameters for optimization of WBW are: G at level 1, I at level 1 and S at level 3 based on results of Table 8.

Table 9 indicates that for resulting in maximum possible DOP, the welding current and welding gap should be considered at their highest levels. Likewise, for achieving lower WBW, welding current and welding gap should be approximately set at their lower ranges.

6. CONCLUSION

In this study the problem of modeling and optimization of A-TIG welding process for AISI316L austenite stainless steel has been addressed. First, A-TIG welding modeling has been

performed based on experimental data gathered as per L_{32} O-A Taguchi method based DOE approach. Major findings drawn from the study are listed below.

1. The process characteristics (*DOP* and *WBW*) as a function of input parameters (welding current, welding speed and welding gap) has been formulated using regression modeling.
2. The most fitted models have been determined based on ANOVA results. Moreover, important parameters and their corresponding percent contribution on each process characteristics has been determined.
3. Based on the results illustrated, welding current is the most important parameter affects *DOP* and *WBW* with 68% and 88% percent contribution respectively. Furthermore, the minor effect belong to welding gap.
4. Taguchi optimization procedure (signal to noise analysis) have been used to optimize the selected models and results confirmed using experimental tests. The result of optimization procedure shows that the proposed method can accurately simulate and optimize the A-TIG welding process authentically (with less than 7% error).

REFERENCES

- [1] H. Y. Huang, S. W. Shyu, K. H. Tseng, C. P. Chou, Evaluation of TIG flux welding on the characteristics of stainless steel, *Journal of Science and Technology of Welding and Joining*, 10(5) (2005) 566–573.
- [2] S. W. Shyu, H. Y. Huang, K. H. Tseng, C. P. Chou, Study of the performance of stainless steel A-TIG welds, *Journal of Materials Engineering and Performance*, 17(2) (2008) 197–201.
- [3] H. Fujii, T.L.U.S.P. Sato, K. Nogi, Development of an advanced A-TIG (AA-TIG) welding method by control of Marangoni convection, *Materials Science and Engineering: A*, 495(7) (2008) 296–303.
- [4] E. Ahmadi, A. R. Ebrahimi, R. A. Khosroshahi, Welding of 304L Stainless Steel with Activated Tungsten Inert Gas Process (A-TIG), *International Journal of ISSI*, 10(1) (2013), 27-33.
- [5] S.P. Lu, D.Z. Li, H. Fujii, K. Nogi, Time dependent weld shape in Ar-O₂ shielded stationary GTA welding, *Journal of Material Science and Technology*, 23(5) (2007) 650–654.
- [6] M. Moradi, M. Ghoreishi, M.J. Torkamany, Modeling and Optimization of Nd: YAG Laser-TIG Hybrid Welding of Stainless Steel, *Journal of lasers in Engineering*, 27(2) (2014) 211–230.
- [7] M. Ragavendran, N. Chandrasekhar, R. Ravikumar, M. Vasudevan, A.K. Bhaduri, Optimization of hybrid laser – TIG welding of 316LN steel using response surface methodology (RSM), *Optics and Lasers in Engineering*, 94(6) (2017) 27-36.
- [8] H.C. Chen, E.L. Ng, Z. Du, Hybrid laser-TIG welding of dissimilar ferrous steels: 10 mm thick low carbon steel to 304 austenitic stainless steel, *Journal of Manufacturing Processes*, 47 (2) (2019) 324-336.
- [9] K.H. Dhandha, V.J. Badheka, Effect of activating fluxes on weld bead morphology of P91 steel bead-on-plate welds by flux assisted tungsten inert gas welding process, *Journal of Material and Manufacturing Processes*, 17(2) (2015) 48–57.
- [10] R.S. Vidyarthi, A. Kulkarni, D.K. Dwivedi, Study of microstructure and mechanical property relationships of A-TIG welded P91-316L dissimilar steel joint, *Materials Science & Engineering A*, 695 (17) (2017) 249-257.
- [11] K.D. Ramkumar, V. Varma, M. Prasad, N.D. Rajan, Effect of activated flux on penetration depth, microstructure and mechanical properties of Ti-6Al-4V TIG welds, *Journal of Materials Processing Tech.* 261(3) (2018) 233–241.
- [12] V. Kumar, B. Lucas, D. Howse, G. Melton, S. Raghunathan, L. Vilarinho, Investigation of the A-TIG Mechanism and the Productivity Benefits in TIG Welding. In JOM-15, *Fifteenth International Conference on the Joining of Materials*, December 2009.
- [13] G. Venkatesan, J. George, M. Sowmyasri, V. Muthupandi, Effect of Ternary Fluxes on Depth of Penetration in A-TIG Welding of AISI 409 Ferritic Stainless Steel, *Procedia Materials Science*, 5(2) (2014) 2402-2410.
- [14] T.S. Chern, K.H. Tseng, H.L. Tsai, Study of the characteristics of duplex stainless steel activated tungsten inert gas welds, *Materials & Design*, 32 (1) (2011) 255-263.
- [15] S. Tathgir, A. Bhattacharya, Activated-TIG welding of different steels: influence of various flux and shielding gas, *Materials and Manufacturing Processes*, 31(3) (2015) 335–342.
- [16] F. Kolahan, M. Azadi Moghaddam, The use of Taguchi method with grey relational analysis to optimize the EDM process parameters with multiple quality characteristics, *Scientia Iranica B*, 22(2) (2015) 530-538.
- [17] R. Pamnani, M. Vasudevan, T. Jayakumar, P. Vasantharaja, Development of Activated Flux, Optimization of Welding Parameters and Characterization of Weld Joint for DMR-249A Shipbuilding Steel, *Transactions of the Indian Institute of Metals*, 70(1) (2017) 49–57.
- [18] G. Venkatesan, V. Muthupandi, J. Justine, Activated TIG welding of AISI 304L using mono- and tri-component fluxes, *The International Journal of Advanced Manufacturing Technology*, 93(1-4) (2017) 329–336.
- [19] K.H. Tseng, C.Y. Hsu, Performance of activated TIG process in austenitic stainless steel welds, *Journal of Materials Processing Technology*, 211(5) (2011) 503–512.
- [20] M. Vishwakarma, V.V.K. Parashar, Regression Analysis and Optimization of Material Removal Rate on Electric Discharge Machine for EN-19 Alloy Steel, *International Journal of Scientific and Research Publications*, 2(11) (2012) 167-175.
- [21] D. Vishnu, R.I. Asal, T. Patel, B. Alok, Optimization of Process Parameters of EDM Using ANOVA Method, *International Journal of Engineering Research and Applications*, 3 (2) (2013) 1119-1125.
- [22] M. Azadi Moghaddam, F. Kolahan, Application of orthogonal array technique and particle swarm optimization approach in surface roughness modification when face milling AISI1045 steel parts, *Journal of Industrial Engineering International*, 12(2) (2016) 199–209.

HOW TO CITE THIS ARTICLE

M. Azadi Moghaddam, F. Kolahan, *Modeling and Optimization of Flux Assisted Tungsten Inert Gas Welding Process Using Taguchi Method and Statistical Analysis*. *AUT J. Mech Eng.*, 4(3) (2020) 415-424.

DOI: 10.22060/ajme.2019.16890.5839



